Original Article

Ultra-wide optical coherence tomography angiography in diabetic retinopathy

Qinqin Zhang[1], Kasra A. Rezaei[2], Steven S. Saraf[2], Zhongdi Chu[1], Fupeng Wang[1], Ruikang K. Wang[1,2]

[1]Department of Bioengineering, University of Washington, Seattle, Washington, USA; [2]Department of Ophthalmology, University of Washington Eye Institute, Seattle, Washington, USA

Correspondence to: Ruikang K. Wang, PhD. Department of Bioengineering, University of Washington, Seattle, WA 98195, USA. Email: wangrk@uw.edu.

Background: To implement an ultra-wide optical coherence tomography angiography imaging (UW-OCTA) modality in eyes with diabetic retinopathy (DR) with the aim of quantifying the burden of microvascular disease at baseline and subsequent clinic visits.

Methods: UW-OCTA was implemented on a 1,060 nm swept source (SS) OCTA engine running at 100 kHz A-line rate with a motion tracking mechanism. A montage scanning protocol was used to capture a 100-degree field of view (FOV) using a 4×4 grid of sixteen total individual 6×6 mm^2 scans. Typical OCTA images with a FOV of 3×3, 6×6 and 12×12 mm^2 were obtained for comparison. DR patients were scanned at baseline and follow-up. They were treated at the clinician's discretion. Vessel density and non-perfusion area maps were calculated based on the UW-OCTA images.

Results: Three proliferative DR patients were included in the study. UW-OCTA images provided more detailed visualization of vascular networks compared to 50-degree fluorescein angiography (FA) and showed higher burden of pathology in the retinal periphery that was not captured by typical OCTA. Neovascularization complexes were clearly detected in the two patients with active PDR. Vessel density and non-perfusion maps were used to measure progressive capillary non-perfusion and regression of neovascularization between visits.

Conclusions: UW-OCTA provides approximately 100-degree OCTA images of the fundus comparable to that of wide-angle fundus photography, and may be more applicable in conditions such as DR which affect the peripheral retina in contrast to standard OCTA.

Keywords: Diabetic retinopathy (DR); field of view (FOV); non-perfusion; optical coherence tomography angiography (OCTA); swept source OCTA; vessel density

Submitted Sep 04, 2018. Accepted for publication Sep 12, 2018.
doi: 10.21037/qims.2018.09.02
View this article at: http://dx.doi.org/10.21037/qims.2018.09.02

Introduction

Diabetic retinopathy (DR) is the leading cause of blindness in the United States for patients aged 20–64 years (1). It is characterized by microaneurysms (MAs), capillary non-perfusion, and ischemia within the retina (2-5) that may lead to several complications, such as diabetic macular edema (DME), diabetic macular ischemia, and neovascularization of the retina (6-10). Capillary non-perfusion impairs the delivery of nutrients to the neuroglial tissues in the retina, resulting in hypoxia and the expression of vascular endothelial growth factor (VEGF). VEGF promotes both angiogenic responses and vascular permeability (11,12). Currently, retinal capillary non-perfusion is readily demonstrated by fluorescein angiography (FA). Midperipheral capillary non-perfusion has been shown to be the most common type in early stage DR and the extent of capillary non-perfusion is more pronounced in eyes with retinal and optic disc neovascularization (13,14). Therefore, it is crucial to detect midperipheral or far peripheral

capillary non-perfusion in DR patients, especially in the early stages of the disease.

FA, a dye-based angiography, is widely recognized as an essential tool in evaluating the severity of DR (15). Traditional fundus cameras capture FA images from the posterior pole, covering a 20–50 degree field which is important for macular diseases such as age-related macular degeneration. The introduction of widefield imaging systems, including color fundus photography and FA, has proven to be of higher utility in diseases such as DR that have significant effects on the peripheral retina (16-18). Compared to the traditional fundus images, widefield FA imaging devices enable imaging of up to 200 degrees of the posterior pole in a single scan. However, despite its clinical usefulness, FA and widefield FA are invasive procedures requiring the intravenous injection of fluorescein which has documented risks of nausea, vomiting, itching, anaphylaxis, and in rare cases, can cause death (19).

Optical coherence tomography (OCT) is a non-invasive imaging modality that can rapidly render three-dimensional images of retinal microanatomy. It has become an important tool in the management of DR, especially with the advent of anti-VEGF therapy for the treatment of DME (20). Optical coherence tomography angiography (OCTA) (21-25) is a further step in OCT technology that allows assessment of the microvasculature by detecting functional blood flow. It has become increasingly important as a non-invasive, functional imaging modality in conditions affecting the retinal and choroidal vasculature (26-29). The basis of OCTA is to isolate and exhibit only tissues with variable backscattering of light. By repeating an OCT scan multiple times at the same location, post-processing methods are applied to isolate only tissues that produce variable backscattering of light such as those produced by the continual flux of red blood cells through the retinal vasculature (30,31). Given current OCT system speed, the tolerance of the human eye to maintain its position for approximately 5 seconds limits the field of view (FOV) obtainable by OCTA, which requires rapid acquisition of images in a small window of time. Typically, 3×3 and 6×6 mm^2 are the most common FOVs of spectral domain (SD) OCTA with an imaging speed of approximately 70 kHz. Larger FOVs of up to 9×9 and 12×12 mm^2 can be achieved in a single scan by utilizing a faster swept source (SS) OCTA system (100 kHz). However, with larger scan areas, there is a correspondingly decreased resolution of the fine retinal vasculature. To maintain the high resolution of the vasculature, a montage protocol can be used to cover a larger FOV, performing multiple individual scans of the fundus and merging them into a larger image. Zhang *et al.* showed that montaged SD-OCTA images could be used to cover a larger FOV of approximately 50 degrees while maintaining a high vascular resolution (32). The described method is comparable to traditional fundus imaging, but still it is not ideal for conditions such as DR that predominately affect the more peripheral retina.

In this study, we implemented a montage protocol that utilizes SS-OCTA to achieve ultra-wide images that are more applicable in DR patients. The more rapid acquisition time of SS-OCTA makes this method possible and practical in the clinical setting.

Methods

Clinical and imaging data were collected prospectively from patients receiving care at the eye institute at the University of Washington, Seattle, WA, between January 2016 and October 2017. This study was approved by the Institutional Review Board of the University of Washington and informed consent was obtained from all subjects. This study followed the tenets of the Declaration of Helsinki and was conducted in compliance with the Health Insurance Portability and Accountability Act.

All patients underwent imaging with a 100 kHz Plex® Elite 9000 SS-OCTA (Carl Zeiss Meditec Inc., USA) machine that operates at a central wavelength of 1,060 nm with a bandwidth of 100 nm, an A-scan depth of 3.0 mm in tissue, a full-width at half maximal (FWHM) axial resolution of approximately 5 µm in tissue, and a lateral resolution at the retinal surface estimated at 12 µm. FastTrac™ motion correction software was used while the images were acquired, which enabled the montage scanning protocol to achieve an unprecedented FOV. The montage was comprised of a 4×4 grid of sixteen total individual 6×6 mm^2 FOV scans. Two repeated B-scans were acquired as a cluster scan at each position over the slow axis. In total, 500 clusters were stepped in the slow axis. In each B-scan, 500 A-lines were sampled over the fast axis direction. The high-density sampling of the 6×6 mm^2 scans resulted in 12 µm spacing, rendering the retinal microvasculature at high resolution and allowing for quantitative analysis. The complex optical microangiography (OMAG^c) algorithm was used to obtain OCTA images, by utilizing the variations in both the intensity and phase information between sequential B-scans at the same location to generate flow signal (30). The 4×4 grid was imaged in a standardized manner by

changing the fixation target to guide the OCT probe. Twenty percent overlap between adjacent cubes was allowed in order to guide the rendering of the montage image. In addition, traditional single scan images were obtained, including 3×3, 6×6 and 12×12 mm^2, to allow comparison with the ultra-wide montage image.

Retinal layers were segmented using a validated semi-automated segmentation algorithm (33). Three retinal layers were segmented in all patients: a vitreous retinal layer (VRL) that is a slab covering approximately 100 microns above the inner limiting membrane (ILM), a superficial retinal layer (SRL) extending from the ILM to the inner plexiform layer (IPL), and a deep retinal layer (DRL) covering a slab from the outer border of the IPL to the outer border of the outer plexiform layer (OPL) (32). Maximum projection was applied on the segmented volumes to generate the en face angiograms. The different layers were color coded as follows: purple in VRL, red in SRL, and green in DRL. An automated montage algorithm was then applied to generate the final ultra-wide angiograms.

Vessel density and flow impairment areas indicating capillary non-perfusion were calculated on the en face angiograms using our previously described method (34).

A non-perfusion flow impairment map was created in all patients to highlight voids where capillaries were not detected but excluding areas of less than or equal to 0.03 mm^2. In addition, the foveal avascular zone and optic disc were excluded in the analysis. Comparisons between the composite ultra-wide FOV and common FOVs in detecting flow impairment area were conducted. In addition, vessel density changes were detected between clinical visits.

Results

Starting from January 2016, 50 patients comprising a total of 60 study eyes with either non-proliferative DR (NPDR) or proliferative diabetic retinopathy (PDR), were enrolled in our study and underwent OCTA imaging. Twelve study eyes were excluded due to severe cataract or motion artifacts. Thirty patients, contributing 20 study eyes, underwent ultra-wide FOV scans. Of these, 3 patients, contributing four study eyes in total, underwent the montage UW-OCTA scan, in addition to the single scan images of all three FOVs (3×3, 6×6 and 12×12 mm^2). These three cases are described in this report. Of note, one of the three patients (patient #3) had an adverse reaction to traditional FA imaging and refused further invasive studies. She was subsequently followed with SS-OCTA scans on her routine clinical visits in order to monitor progression.

Patient #1: PDR (non-high risk) in a 33-year-old man

A 33-year-old man presented with best-corrected visual acuity (BCVA) of 20/20 in the right eye and was diagnosed with non-high risk PDR. Both color fundus photography and traditional FA images demonstrated intraretinal hemorrhages and MAs in the macula (*Figure 1A,B*). Typical 3×3 mm^2 (*Figure 1C*) and 6×6 mm^2 (*Figure 1D*) OCTA images showed only details of the central macula and did not provide a FOV comparable to traditional fundus imaging, but did provide greater detail of the capillary networks in the macula. A 12×12 mm^2 (*Figure 1E*) OCTA image encompassed the macula and a portion of the retina outside of the arcades, but with lower resolution of the capillary networks compared to the smaller FOV scans. The UW-OCTA image (*Figure 1F*), with approximately 100 degrees FOV, demonstrated the widest field view with vascular detail comparable to the smaller FOV scans. The UW-OCTA demonstrated non-perfusion areas (dark signal), and neovascularization in the VRL (purple color) that were not visualized on traditional FA or the smaller field OCTA scans.

Quantification methods previously described (34) were applied to the UW-OCTA image to quantify the areas of non-perfusion as well as vessel density (*Figure 2*). Flow impairment was found to be more concentrated in the retinal periphery rather than the macula (area shaded green in *Figure 2C*) with less dense capillary circulation in the same distribution (*Figure 2D*). To provide quantitative measures, we measured the non-perfusion areas with typical 50-degree FA FOV (yellow dashed circle in *Figure 2C*), and compared that to the outside region within 100-degree OCTA. The total area of non-perfusion was 11.83 mm^2 within 50-degree FOV, whereas that of the outside 50-degree but within 100-degree FOV, was 108.59 mm^2.

Patient #2 inactive PDR in a 54-year-old man

A 54-year-old man presented with best-corrected visual acuity (BCVA) of 20/20 in his left eye that was stable compared to 1 year ago. Panretinal photocoagulation (PRP) had been performed in the left eye 20 years ago with scars demonstrated on both the typical 50-degree color fundus photograph (*Figure 3A*) and FA (*Figure 3B*) images. The UW-OCTA images at baseline and his subsequent follow up 1 year later are shown in *Figure 3C,D,E* and *Figure 3F,G,H,*

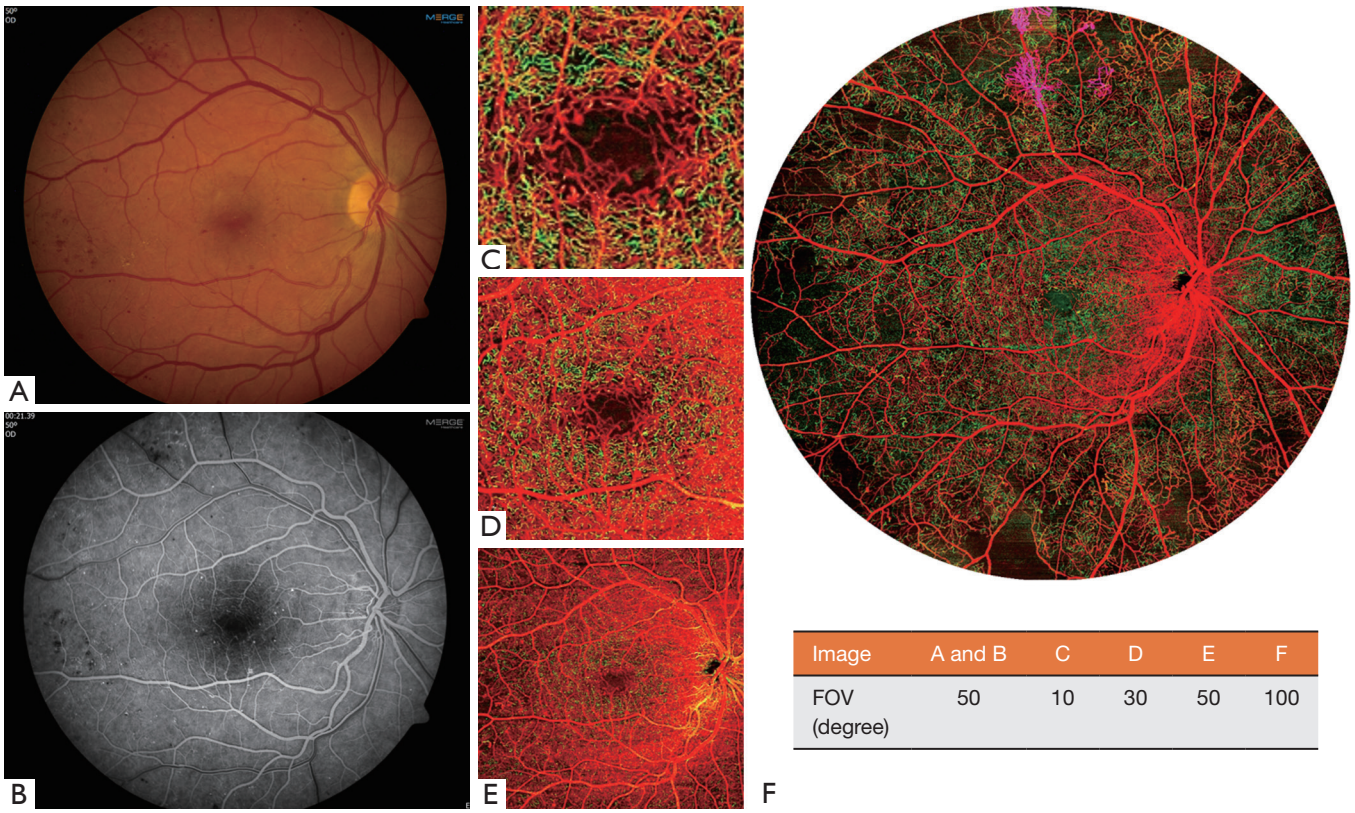

Image	A and B	C	D	E	F
FOV (degree)	50	10	30	50	100

Figure 1 The clinical images and OCTA images with different field of views (FOVs) of a 33-year-old man (patient #1) with a diagnosis of non-high risk PDR in his right eye. (A) 50-degree color fundus image; (B) 50-degree early phase of FA image; (C,D,E) typical OCTA color-coded images with a FOV of 3×3, 6×6, and 12×12 mm^2 scans, respectively; (F) the ultra-wide OCTA color-coded image with a FOV of approximately 100 degrees. Red indicates superficial retinal layer (SRL); Green indicates deep retinal layer (DRL); Purple indicates the vitreous retinal layer (VRL) to demonstrate neovascularization consistent with PDR. The FOVs of each image are listed in the table.

respectively. A 50-degree circle is overlaid onto the UW-OCTA images demonstrating the additional information gained by widefield OCTA compared to traditional fundus camera images. Quantitative measures of non-perfusion area in *Figure 3D* and *Figure 3G* within typical 50-degree FOV were 9.68 mm^2 for the first visit and 10.38 mm^2 for the second visit, respectively. However, these values were 67.36 mm^2 for the first visit and 69.88 mm^2 for the second visit in the region bounded by 50-degree and 100-degree outlines. The vessel density maps in *Figure 3E,H* showed that there is no appreciable difference in the 1-year follow-up interval (on average 24.42% *vs.* 24.77%), suggesting stable or minimal progressive capillary perfusion loss.

Patient #3 High-risk PDR in a 31-year-old woman

A 31-year-old woman presented with best-corrected visual acuity (BCVA) of 20/20 in her right eye and 20/60 in her left eye. At her initial consultation, the patient had a severe allergic reaction to the fluorescein dye and fainted. She did not consent to further FA studies. However, Optos widefield color fundus images were captured on both right and left eyes (*Figure 4*). Her baseline UW-OCTA showed extensive neovascularization of the disc (NVD) and retina elsewhere (NVE) in the left eye (*Figure 5A*). Intravitreal bevacizumab and panretinal photocoagulation laser treatments were performed in the left eye. One month later, the UW-OCTA was repeated (*Figure 5B*). Comparison of Optos photograph (*Figure 4A*) to UW-OCTA (*Figure 5*) demonstrates the response to treatment more dramatically in the color-coded UW-OCTA, showing regression of the NVD and NVE. The non-perfusion map (*Figure 5C,D*) reflects the regression of neovascularization in the VRL, exposing a larger area of underlying non-perfusion in the

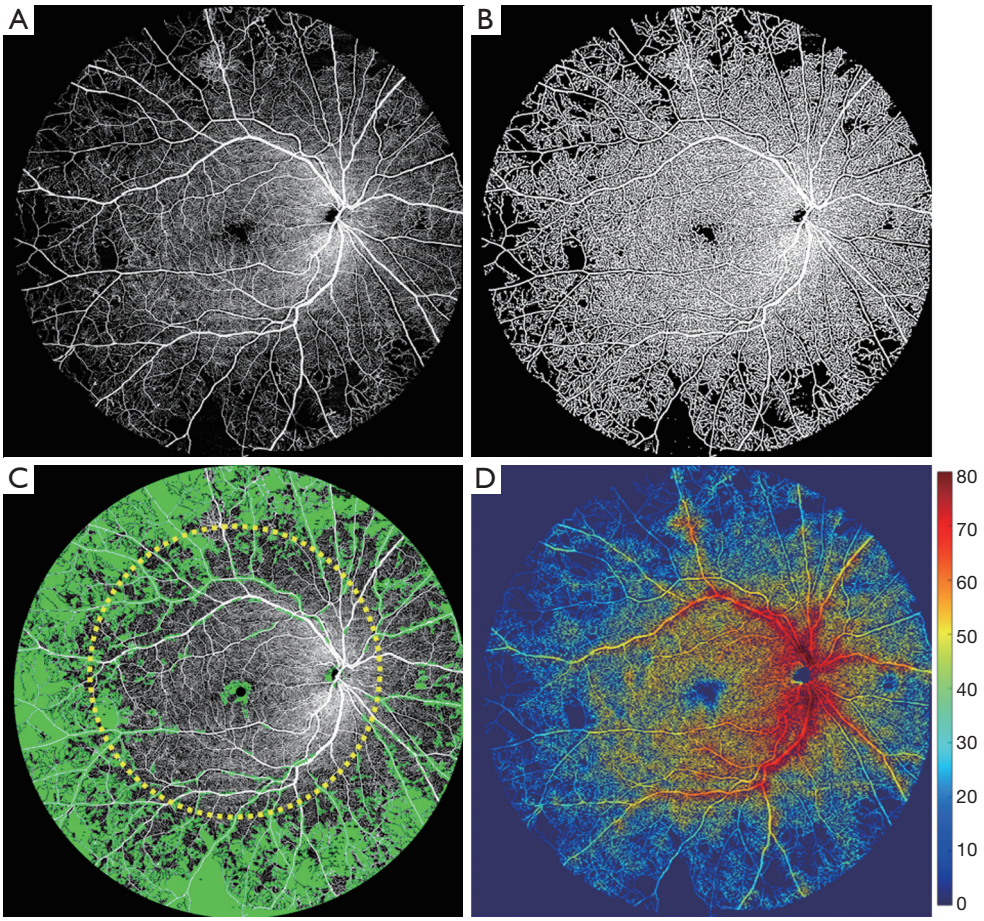

Figure 2 Ultra-wide OCTA image of the whole retinal layer (WRL) in gray scale of patient #1 and the corresponding quantification process. (A) The original ultra-wide OCTA image; (B) binary OCTA image that was used for vessel density and further non-perfusion area measurements; (C) the OCTA image overlaid with non-perfusion area map in green color. Typical 50-degree FOV is outlined approximately with yellow dashed circle. The non-perfusion area within the outlined circle is measured with 11.83 mm^2, whereas that of the outside is 108.59 mm^2. (D) The vessel density map overlaid with the binary OCTA image. The color-bar indicates the degree of the vessel density in percentage.

retinal circulation. Quantitative measures of total non-perfusion area in *Figure 5C,D* within typical 50-degree FOV were 32.31 mm^2 for the first visit and 49.02 mm^2 for the second visit, respectively. The non-perfusion in the area bounded by the 50-degree and 100-degree lines was 122.37 mm^2 at the first visit, and 135.84 mm^2 for the second visit. The vessel density maps in *Figure 5E,F* showed that there is also a decrease in the vessel density measurement by the second visit (30.26% to 22.02% on average) consistent with the regression of NVD and NVE.

Figure 6 shows images of the patient's right eye. Again, the NVD and NVE are more readily appreciable on the UW-OCTA images compared to the Optos image. With one month of observation, the NVE has progressed in the UW-OCTA image (*Figure 6A vs. Figure 6D*) and on the vessel density map [*Figure 6C* (27.52% in average) *vs. Figure 6F* (24.69% in average)]. Non-perfusion area (*Figure 6B vs. Figure 6E*) has also progressed within the 50-degree FOV (30.28 to 35.91 mm^2), but more so outside of the 50-degree region (84.71 to 97.77 mm^2).

Discussion

In this study, we utilized SS-OCTA in a novel protocol to render UW-OCTA images in patients with PDR. As we showed in our previous study, the maximum composited

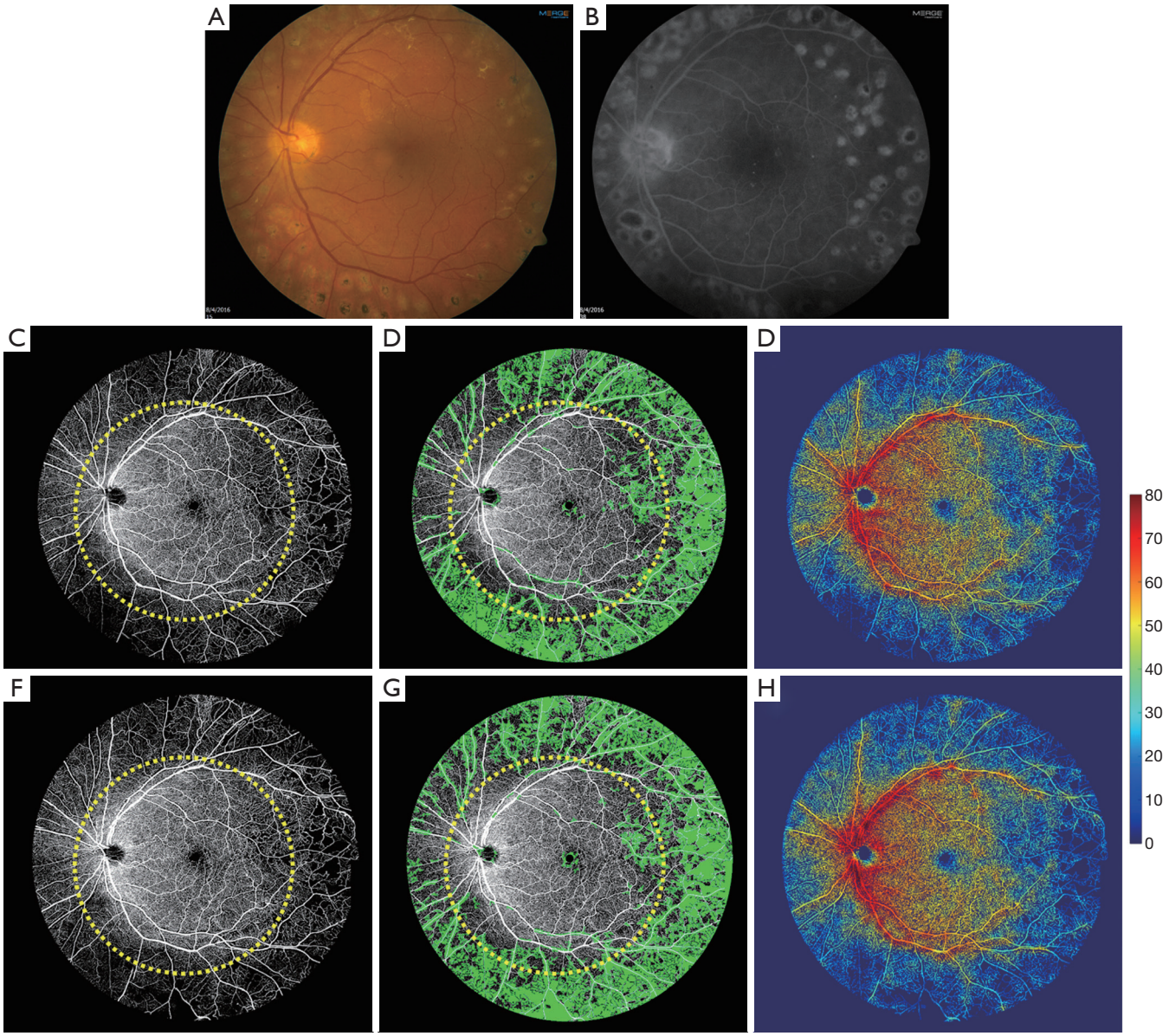

Figure 3 Clinical images and ultra-wide OCTA images of a 54-year-old man (patient #2) with a diagnosis of inactive PDR on his left eye. The clinical images were taken in his first visit. (A) 50-degree color fundus image; (B) 50-degree late phase of FA image; (C,F) the original ultra-wide OCTA images at his baseline and 1-year follow-up visit; (D,G) the non-perfusion map in green color of his first and follow-up visit; (E,H) vessel-density map overlaid with binary map of the two different visits. The yellow circle overlaid on OCTA images is a 50-degree circle to identify the typical clinical FOV.

FOV on patients we obtained from the SD-OCTA prototype with an A-line rate of 68 kHz can be extended to 50 degrees with high vascular resolution (contributed by the dense sampling of the single cube, 2.4×2.4 mm^2 with 245 A-line × 245 B-scan), comparable to the standard clinical images. In this study, the faster speed of SS-OCTA (up to 100 kHz) and its modified tracking system allowed us to extend the FOV even wider to approximately 100 degrees with less imaging time. The application of this methodology is of special interest in cases such as DR and other retinal conditions predominately affecting the peripheral retina, such as sickle cell retinopathy, retinal vasculitis, or ocular

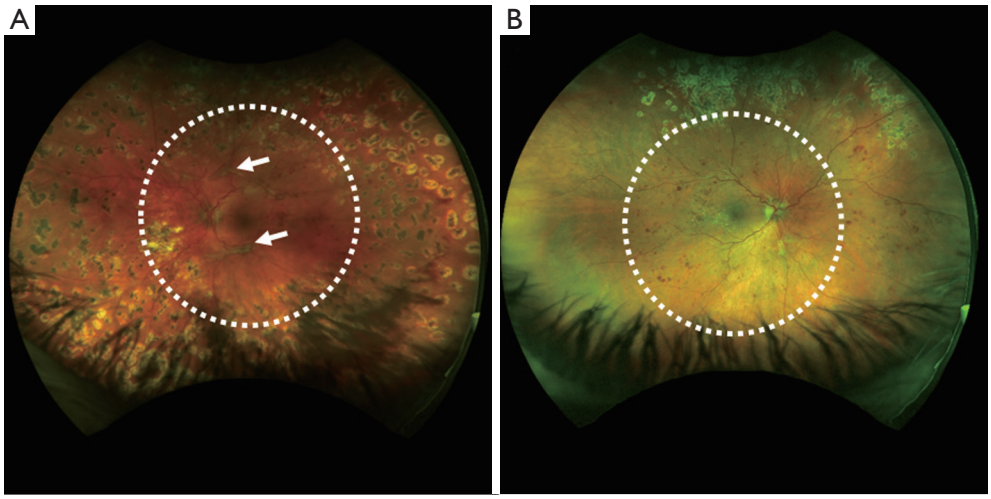

Figure 4 Optos ultra-wide color fundus image of a 31-year-old female (patient #3) with a diagnosis of (A) severe PDR on her left eye and (B) PDR on her right eye. Typical 50-degree FOV is outlined with white dashed circle line.

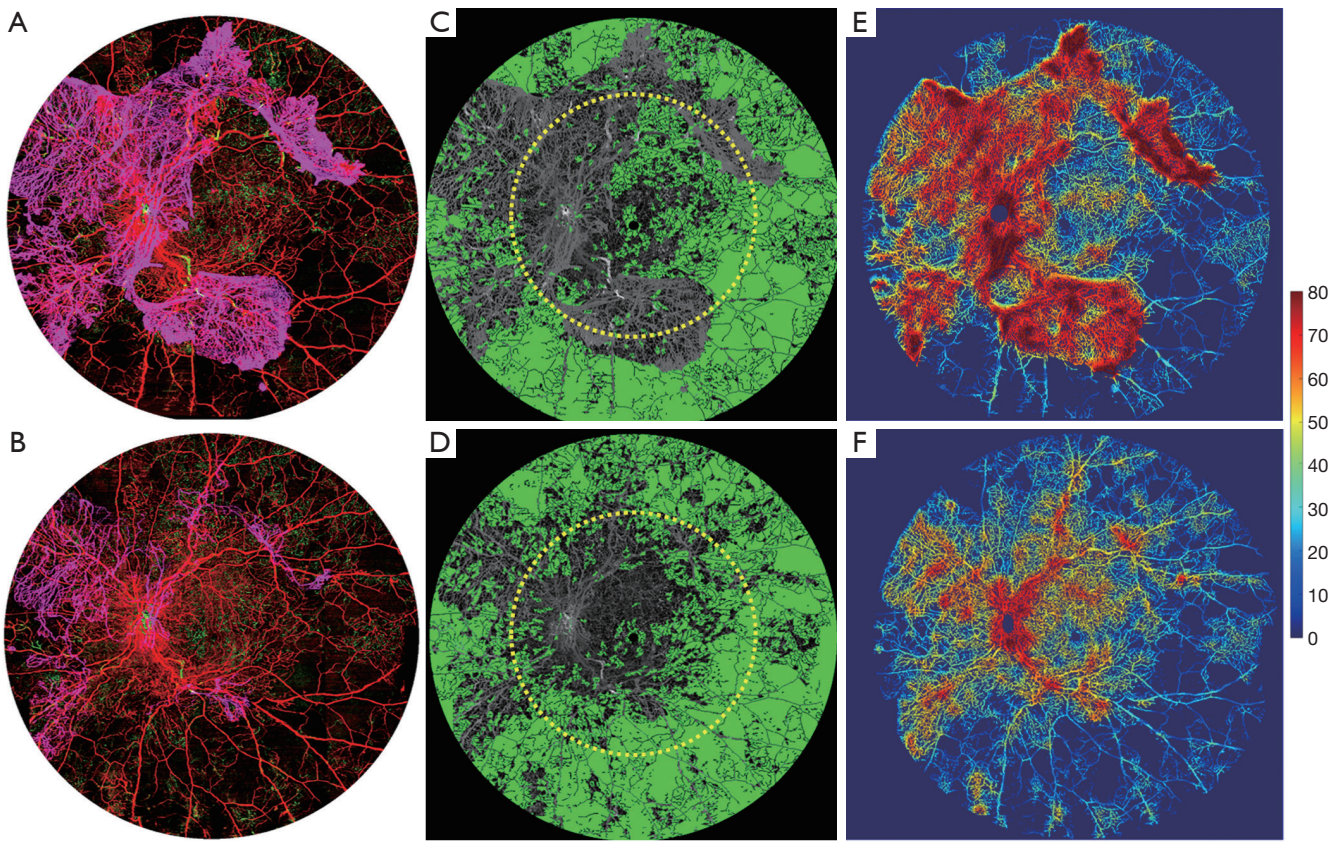

Figure 5 Ultra-wide OCTA image of a 31-year-old woman (patient #3) with a diagnosis of severe PDR on her left eye. (A,B) Ultra-wide color-coded OCTA images at the first visit and 1-month follow-up visit after intravitreal bevacizumab and panretinal photocoagulation; (C,D) the non-perfusion map in green color of his first and second visit; (E,F) vessel density map of her first and second visit. The yellow circle overlaid on OCTA images is a 50-degree circle to identify the typical clinical FOV. On (A) and (E), red indicates superficial retinal layer (SRL); green indicates deep retinal layer (DRL); purple indicates the vitreous retinal layer (VRL) to demonstrate the neovascularization.

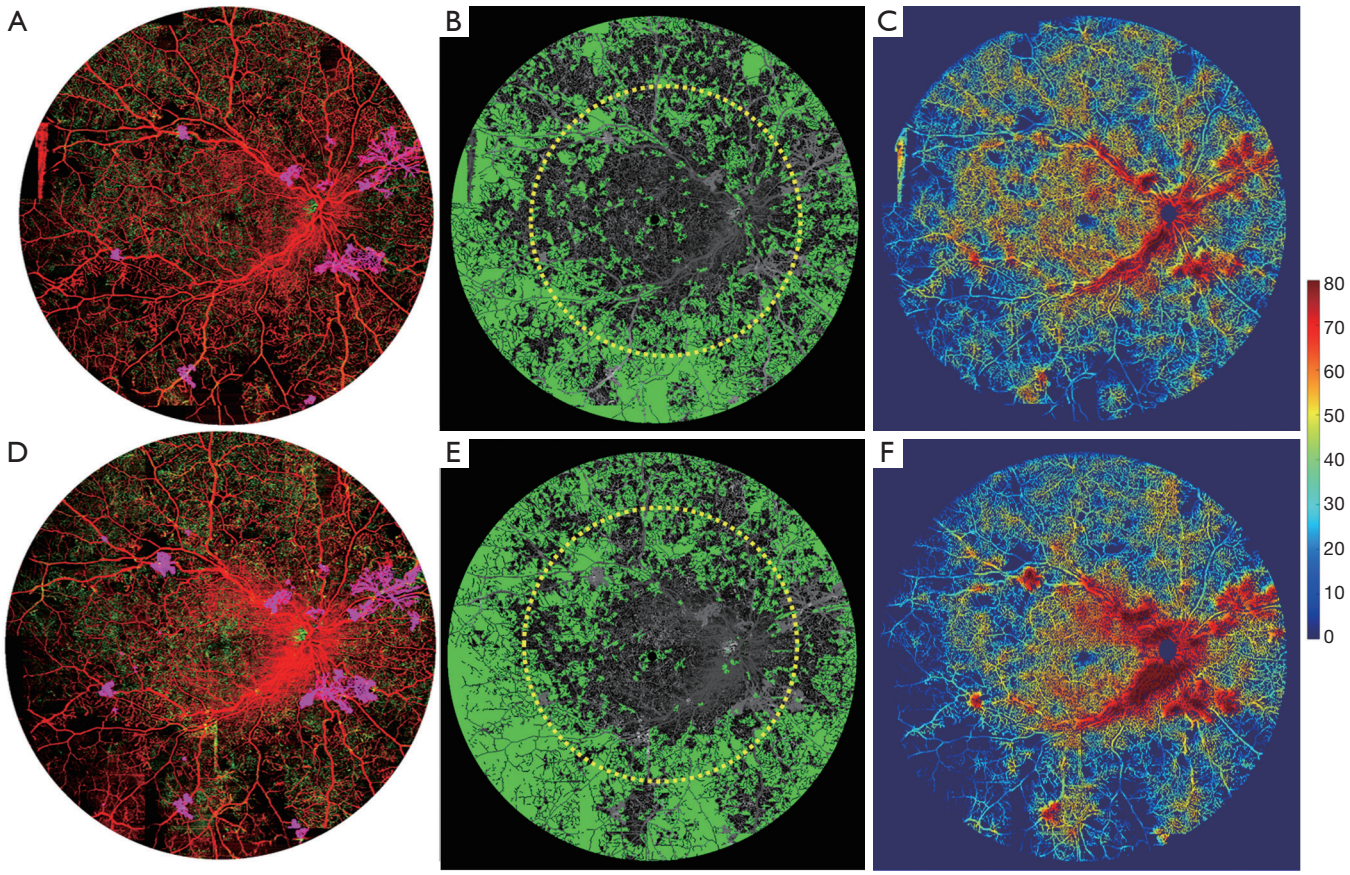

Figure 6 Ultra-wide OCTA image of a 31-year-old woman (patient #3) with a diagnosis of PDR in her right eye. (A,D) Ultra-wide color-coded OCTA images of the first visit and one-month follow-up visit; (B,E) the non-perfusion map in green color of his first and second visit; (C,F) Vessel-density map at her baseline and 1 month follow-up visit. The yellow circle overlaid on OCTA images is a 50-degree circle to identify the typical clinical FOV. On (A) and (D), red indicates superficial retinal layer (SRL); Green indicates deep retinal layer (DRL); Purple indicates the vitreous retinal layer (VRL) to demonstrate the neovascularization.

ischemic syndrome.

The three reported cases demonstrate the ability of UW-OCTA to provide valuable clinical information in grading retinopathy, monitoring stability, or monitoring treatment response.

In the case of patient #1, it is clear that OCTA renders a higher level of capillary network detail compared to conventional FA. Furthermore, the wider FOV of UW-OCTA captured NVE missing in the 50-degree image obtained by traditional FA and the smaller FOV OCTA scans (*Figure 1C,D,E*). In the case of patient #2, the patient had a history of inactive PDR. UW-OCTA showed no active NVD or NVE and capillary density remained stable at 1-year follow-up, corresponding to the assessment of clinical stability. In the case of patient #3, we presented a case of adverse reaction to fluorescein dye that was effectively followed with the less invasive UW-OCTA. In this case, we are able to monitor the response of NVD and NVE to intravitreal anti-VEGF injections and PRP without invasive fluorescein dye testing. It can also be concluded that regression of NVD and NVE after treatment is more easily appreciated with UW-OCTA compared to Optos fundus photography. UW-OCTA may be of significant value in such clinical contexts wherein the number of necessary injections to achieve control requires frequent re-imaging, such as when more providers are opting to treat PDR with anti-VEGF injections rather than PRP (35,36). In the fellow eye, quantification indices on the vessel-density map show worsening NVE in the right eye after 1-month observation. In addition, progressive non-perfusion was measured on

the non-perfusion map. All three cases demonstrate that the burden of microangiopathy in DR is more heavily concentrated outside of the central 50 degrees that are captured by conventional photography methods.

There are limitations in our methodology. First, the acquisition time of UW-OCTA imaging is relatively long compared to standard OCTA imaging, which takes approximately 5 seconds per scan. Each UW-OCTA takes around 20 minutes to perform for both eyes, which may make acquisition difficult in patients who have low vision and cannot maintain fixation. On the other hand, acquisition time and difficulty may be comparable or better when compared to standard FA, which requires significant set-up time, placement of intravenous access, and at least 10 minutes of image capture time, exposing the patient to significant flash photography. Second, we provide quantification of retinal capillary perfusion using a vessel-density map. Although this may allow trending of microvascular disease between visits, there have not been studies to establish the clinical significance of vessel density changes. Most of our understanding and clinical approach to DR are from clinical findings such as MAs, retinal hemorrhages, and signs of neovascularization, which have been described in the ETDRS study. Further study is needed to understand the clinical utility of vessel density changes now that advancements in technology make trending this metric possible.

In summary, we have described an ultra-wide OCTA imaging protocol for DR patients, which can provide up to 100 degrees of high vascular resolution by utilizing SS-OCTA. The UW-OCTA images capture both the entire macula and retinal periphery in DR patients, which has widespread application in early disease screening, assessing treatment response, and assessing stability.

Acknowledgements

Funding: Research supported by grants from Carl Zeiss Meditec, Inc. (Dublin, CA), the National Eye Institute (R01EY024158, R01EY028753), an unrestricted grant from the Research to Prevent Blindness, Inc., New York, NY, and the Washington Research Foundation. The funding organization had no role in the design or conduct of this research.

Footnote

Conflicts of Interest: Dr. Wang disclosed intellectual property owned by the Oregon Health and Science University and the University of Washington related to OCT angiography, and licensed to commercial entities, which are related to the technology and analysis methods described in parts of this manuscript. Dr. Wang received an innovative research award from Research to Prevent Blindness. He is a consultant to Carl Zeiss Meditec, and Insight Photonic Solutions.

Ethical Statement: This study was approved by the Institutional Review Board of the University of Washington and informed consent was obtained from all subjects. This study followed the tenets of the Declaration of Helsinki and was conducted in compliance with the Health Insurance Portability and Accountability Act.

References

1. Klein R, Klein BE, Moss SE, Davis MD, DeMets DL. The Wisconsin epidemiologic study of diabetic retinopathy. III.Prevalence and risk of diabetic retinopathy when age at diagnosis is 30 or more years. Arch Ophthalmol 1984;102:527-532.
2. Adhi M, Brewer E, Waheed NK, Duker JS. Analysis of morphological features and vascular layers of choroid in diabetic retinopathy usingspectral-domain optical coherence tomography. JAMA Ophthalmol 2013;131:1267-74.
3. Hwang TS, Gao SS, Liu L, Lauer AK, Bailey ST, Flaxel CJ, Wilson DJ, Huang D, Jia Y. Automated quantification of capillary nonperfusion using optical coherence tomography angiography in diabetic retinopathy. JAMA Ophthalmol 2016;134:367-73.
4. Hwang TS, Jia Y, Gao SS, Bailey ST, Lauer AK, Flaxel CJ, Wilson DJ, Huang D. Optical coherence tomography angiography features of diabetic retinopathy. Retina 2015;35:2371-6.
5. Ishibazawa A, Nagaoka T, Takahashi A, Omae T, Tani T, Sogawa K, Yokota H, Yoshida A. Optical coherence tomography angiography in diabetic retinopathy: a prospective pilot study. Am J Ophthalmol 2015;160:35-44.e1.
6. Diabetic Retinopathy Clinical Research Network, Elman MJ, Aiello LP, Beck RW, Bressler NM, Bressler SB, Edwards AR, Ferris FL 3rd, Friedman SM, Glassman AR, Miller KM, Scott IU, Stockdale CR, Sun JK. Randomized trial evaluating ranibizumab plus prompt or deferred laser or triamcinolone plus prompt laser for diabetic macular edema. Ophthalmology 2010;117:1064-1077.e35.

7. Agemy SA, Scripsema NK, Shah CM, Chui T, Garcia PM, Lee JG, Gentile RC, Hsiao YS, Zhou Q, Ko T, Rosen RB. Retinal vascular perfusion density mapping using optical coherence tomography angiography in normals and diabetic retinopathy patients. Retina 2015;35:2353-63.
8. Conrath J, Giorgi R, Raccah D, Ridings B. Foveal avascular zone in diabetic retinopathy: quantitative vs qualitative assessment. Eye (Lond) 2005;19:322-6.
9. ETDRS Research Group. Classification of diabetic retinopathy from fluoresceinangiograms. Early treatment diabetic retinopathy study report number 11. Ophthalmology 1991;98:807-22.
10. ETDRS Research Group. Photocoagulation for diabetic macular edema. Early treatment diabetic retinopathy study report number 1. Arch Ophthalmol 1985;103:1796-806.
11. Aiello LP, Avery RL, Arrigg PG, Keyt BA, Jampel HD, Shah ST, Pasquale LR, Thieme H, Iwamoto MA, Park JE, Nguyen HV, Aiello LM, Ferrara N, King GL. Vascular endothelial growth factor in ocular fluid of patients with diabetic retinopathy and other retinal disorders. N Engl J Med 1994;331:1480-7.
12. Antonetti DA, Klein R, Gardner TW. Diabetic retinopathy. N Engl J Med 2012;366:1227-1239.
13. Niki T, Muraoka K, Shimizu K. Distribution of capillary nonperfusion in early-stage diabetic retinopathy. Ophthalmology 1984;91:1431-9.
14. Shimizu K, Kobayashi Y, Muraoka K. Midperipheral fundus involvement in diabetic retinopathy. Ophthalmology 1981;88:601-12.
15. Classification of diabetic retinopathy from fluorescein angiograms. ETDRS report number 11. Early Treatment Diabetic Retinopathy Study Research Group. Ophthalmology 1991;98:807-822.
16. Wessel MM, Aaker GD, Parlitsis G, Cho M, D'Amico DJ, Kiss S. Ultra-wide-field angiography improves the detection and classification of diabetic retinopathy. Retina 2012;32:785-91.
17. Silva PS, Cavallerano JD, Sun JK, Soliman AZ, Aiello LM, Aiello LP. Peripheral lesions identified by mydriatic ultrawide field imaging: distribution and potential impact on diabetic retinopathy severity. Ophthalmology 2013;120:2587-95.
18. Tan CS, Sadda SR, Hariprasad SM. Ultra-wide retinal imaging in the management of diabetic eye diseases. Ophthalmic Surg Lasers Imaging Retina 2014;45:363-6.
19. Yannuzzi LA, Rohrer KT, Tindel LJ, Sobel RS, Costanza MA, Shields W, Zang E. Fluorescein angiography complication survey. Ophthalmology 1986;93:611-7.
20. American Academy of Ophthalmology: American Academy of Ophthalmology Retina and Vitreous Panel. Preferred Practice Pattern® guidelines. Diabetic retinopathy. San Francisco, CA: American Academy of Ophthalmology; 2014.
21. Deegan AJ, Wang W, Men SJ, Li YD, Song SZ, Xu JJ, Wang RK. Optical Coherence Tomography Angiography Monitors Human Cutaneous Wound Healing Over Time. Quant Imaging Med Surg 2018;8:135-50.
22. Chen CL, Bojikian KD, Zhang QQ, Gupta D, Wen JC, Xin C, Mudumbai RC, Kono R, Johnstone MA, Chen PP, Wang RK. Optic disc perfusion in normal eyes and eyes with glaucoma using optical coherence tomography-based microangiography. Quant Imaging Med Surg 2016;6:125-33.
23. Chen CL, and Wang RK. Optical Coherence Tomography Based Angiography. Biomedical Optics Express 2017;8:1056-82.
24. Kashani AH, Chen CL, Gahm JK, Zheng F, Richter GM, Rosenfeld PJ, Shi Y, Wang RK. Optical coherence tomography angiography: A comprehensive review of current methods and clinical applications. Progress in Retinal and Eye Research 2017;60:66-100.
25. Zhang A, Zhang QQ, Chen CL, Wang RK. Methods and Algorithms for Optical Coherence Tomography Based Angiography: A Review and Comparison. J Biomed Opt 2015;20:100901.
26. Thorell MR, Zhang QQ, Huang Y, An L, Durbin MK, Laron M, Sharma U, Stetson PF, Gregori G, Wang RK, and Rosenfeld PJ. Swept-Source OCT Angiography of Macular Telangiectasia Type 2. Ophthalmic Surg. Lasers Imaging Retina 2014;45:369-80.
27. Kim DY, Fingler J, Zawadzki RJ, Park SS, Morse LS, Schwartz DM, Fraser SE, Werner JS. Optical imaging of the chorioretinal vasculature in the living human eye. Proc Natl Acad Sci U S A 2013;110:14354-9.
28. Zhang Q, Wang RK, Chen CL, Legarreta AD, Durbin MK, An L, Sharma U, Stetson PF, Legarreta JE, Roisman L, Gregori G, Rosenfeld PJ. Swept source OCT angiography of neovascular MacTel2. Retina 2015;35:2285-99.
29. Roisman L, Zhang Q, Wang RK, Gregori G, Zhang A, Chen CL, Durbin MK, An L, Stetson PF, Robbins G, Miller A, Zheng F, Rosenfeld PJ. Optical Coherence Tomography Angiography of Asymptomatic Neovascularization in Intermediate Age-Related Macular Degeneration. Ophthalmology 2016;123:1309-19.
30. Wang RK, An L, Francis P, Wilson DJ. Depth-resolved

imaging of capillary networks in retina and choroid using ultrahigh sensitive optical microangiography. Opt Lett 2010;35:1467-9.
31. Wang RK. Optical Microangiography: A Label Free 3D Imaging Technology to Visualize and Quantify Blood Circulations within Tissue Beds in vivo. IEEE J Sel Top Quantum Electron 2010;16:545-54.
32. Zhang Q, Lee CS, Chao J, Chen CL, Zhang T, Sharma U, Zhang A, Liu J, Rezaei K, Pepple KL, Munsen R, Kinyoun J, Johnstone MA, Van Gelder RN, Wang RK. Wide-field optical coherence tomography based microangiography for retinal imaging. Sci Rep 2016;6:22017.
33. Yin X, Chao JR, Wang RK. User-guided segmentation for volumetric retinal optical coherence tomography images. J Biomed Opt 2014;19:086020.
34. Chu Z, Lin J, Gao C, Xin C, Zhang Q, Chen C, Roisman L, Gregori G, Rosenfeld PJ, Wang RK. Quantitative assessment of the retinal microvasculature using optical coherence tomography angiography. J Biomed Opt 2016;21:66008.
35. Hutton DW, Stein JD, Bressler NM, Jampol LM, Browning D, Glassman AR; Diabetic Retinopathy Clinical Research Network. Cost-effectiveness of intravitreous ranibizumab compared with panretinal photocoagulation for proliferative diabetic retinopathy:secondary analysis from a Diabetic Retinopathy Clinical Research Network randomized clinical trial. JAMA Ophthalmol 2017;135:576-84.
36. Writing Committee for the Diabetic Retinopathy Clinical Research Network, Gross JG, Glassman AR, Jampol LM, Inusah S, Aiello LP, Antoszyk AN, Baker CW, Berger BB, Bressler NM, Browning D, Elman MJ, Ferris FL 3rd, Friedman SM, Marcus DM, Melia M, Stockdale CR, Sun JK, Beck RW. Panretinal photocoagulation vs. intravitreous ranibizumab for proliferative diabetic retinopathy: A randomized clinical trial. JAMA 2015;314:2137-46.

Cite this article as: Zhang Q, Rezaei KA, Saraf SS, Chu Z, Wang F, Wang RK. Ultra-wide optical coherence tomography angiography in diabetic retinopathy. Quant Imaging Med Surg 2018;8(8):743-753. doi: 10.21037/qims.2018.09.02

